SIMULATION OF SEMICONDUCTOR DEVICES AND PROCESSES Vol. 5
Edited by S. Selberherr, H. Stippel, E. Strasser – September 1993

Three-Dimensional Implementation of a Unified Transport Model

A. Pierantoni, A. Liuzzo, P. Ciampolini†, and G. Baccarani

Dipartimento di Elettronica, Informatica e Sistemistica, Università di Bologna
Viale Risorgimento 2, I-40136 Bologna, ITALY
†Istituto di Elettronica, Università di Perugia
I-06131 Santa Lucia-Canetola, Perugia, ITALY

Abstract

This paper describes a unified transport model which self-consistently accounts for thermal effects and hot-carrier phenomena. Such result is achieved by including the energy balance equations for electrons, holes and lattice. The model has been incorporated into the three-dimensional device simulator HFIELDS-3D and its numerical efficiency is tested by simulating both unipolar and bipolar devices.

1. The physical model

The behavior of submicron devices is influenced by complex interactions among non-stationary phenomena, device self-heating, as well as fringing and proximity effects. In principle, therefore, such effects have to be self-consistently described within a unified framework: at present, however, only a few attempts to exploit such a model have been reported, mainly because of the computational burden associated with it. For this reason, Szeto and Reif [1], as well as Benvenuti *et al.* [2], limited themselves to one-dimensional analyses, whereas Katayama and Toyabe [3] developed a three-dimensional, finite-difference discretization scheme.

We present the inclusion of a generalized transport model into the more versatile environment provided by HFIELDS-3D, and compare the efficiency of some solution schemes. The model originates from the three BTEs which describe the dynamics of three interacting subsystems: namely electrons, holes and phonons. Energy-balance equations are obtained by taking the moments of order two of the BTEs:

$$\frac{\partial W_{n,p}}{\partial t} + \operatorname{div} \vec{S}_{n,p} = \vec{F} \cdot \vec{J}_{n,p} + \left(\frac{\partial W_{n,p}}{\partial t} \right)_{coll} \tag{1}$$

$$\frac{\partial W_L}{\partial t} + \operatorname{div} \vec{S}_L = \left(\frac{\partial W_L}{\partial t} \right)_{coll} \tag{2}$$

In the above equations, W represents the energy density and $\vec{S}$ the energy flow, defined as follows:

$$\vec{S}_{n,p} = -\kappa_{n,p} \operatorname{grad} T_{n,p} \mp \left(\frac{5}{2} - s\right) \frac{k_B T_{n,p}}{q} \vec{J}_{n,p} \tag{3}$$

$$\vec{S}_L = -\kappa_L \operatorname{grad} T_L \tag{4}$$

while the current densities $\vec{J}$ are given by:

$$\vec{J}_n = q\mu_n \left[\frac{k_B T_n}{q} \operatorname{grad} n + n \operatorname{grad}\left(\frac{k_B T_n}{q} - \varphi\right)\right] \tag{5}$$

$$\vec{J}_p = -q\mu_p \left[\frac{k_B T_p}{q} \operatorname{grad} p + p \operatorname{grad}\left(\frac{k_B T_p}{q} + \varphi\right)\right] \tag{6}$$

The collision terms, which account for the interactions among different subsystems, are described according to the relaxation-time approximation and fulfill the following relationship:

$$\left(\frac{\partial W_L}{\partial t}\right)_{coll} + \left(\frac{\partial W_n}{\partial t}\right)_{coll} + \left(\frac{\partial W_p}{\partial t}\right)_{coll} = E_G U \tag{7}$$

Finally, the model is completed by Poisson's and current-continuity equations. Spatial discretization is carried out by the Box Integration Method (in analogy with the scheme presented in [4]) applied to the hybrid mesh suggested by Conti *et al.* [5].

2. Simulation results

In this section, the simulation of two simple devices is discussed: namely, the MOSFET shown in Fig. 1 and the BJT shown in Fig. 2 are considered. In both cases, comparisons among several transport models are carried out; more specifically, the following schemes are used: the standard drift-diffusion model (DD), the hydrodynamic model (HD) described in [4], the electrothermal (ET) model introduced in [6] and, finally, the "generalized" thermal-hydrodynamic (TH) model illustrated so far. Contour lines in Figs. 1 and 2 refer to the lattice temperature predicted by the TH model. Fig. 3 compares the MOSFET output characteristics predicted by the different models which exhibit some non-negligible discrepancies. In the low V_{DS} range, neither carrier nor lattice heating occurs, so that predictions given by the four models agree well; at intermediate V_{DS} values, carriers may attain energies well in excess of their equilibrium values, while no lattice heating occurs: HD and TH models consistently predict higher drain currents than DD and ET, due to the carrier velocity overshoot. Eventually the lattice heats up as well, thus resulting in increased lattice scattering probability; the $I_D^{(ET)}$ and $I_D^{(HT)}$ curves deviate downward, with respect to the corresponding isothermal models.

Fig. 4 illustrates the BJT turn-on characteristics: again a fairly large spreading of simulation results is found, depending on the model employed. Basically, carrier and lattice heating occur at the collector, reverse-biased junction, whereas a moderate cooling-down of the carriers can be observed at the emitter junction. In the simulated conditions, impact ionization phenomena play no significant role and are neglected. Thus, little influence of the carrier heating over the collector current is found, being the latter dominated by the cold carriers injected at the emitter. Consistently, the DD and HD predictions are fairly close: differences are mainly to be ascribed to the thermoelectric field appearing in Eqs. (5, 6). Lattice heating, instead, has a substantially larger impact on the characteristics, which is basically due to the increase of the minority carrier density in the base region.

3. Numerical strategies

A truly three-dimensional problem usually requires a large number of meshpoints, which makes it unpractical using a Newton-Raphson solution scheme. A block Gauss-Seidel scheme, analogous to the classical Gummel procedure, has thus necessarily to be used, which calls for a partition of the model equations and the unknown variables into separate sets. Table 1 illustrates our findings about different partitioning strategies: computational performances are compared, for the single-carrier case, assuming the plain DD scheme as a reference. In the second column, the abbreviations POI, ECC, LEB and EEB stand for the set of algebraic equations arising from the discretization of Poisson's equation, of the electron current-continuity equation, of the lattice energy balance and of the electron energy balance, respectively. The three-block TH scheme is simply obtained by supplementing the HD scheme with the decoupled solution of the LEB equation: however, due to the strong coupling among carrier and lattice temperatures, the convergence of such a simplistic algorithm turns out to be unacceptably slow. We found the two-block TH scheme to be much more effective: actually, in the unipolar case, by solving LEB and EEB in a coupled fashion, the computational overhead required by the model can be as low as 25 %, compared with the more traditional hydrodynamic solution. From a qualitative standpoint, similar results are exhibited by the bipolar transistor simulation, as shown in table 2[1]: in this case, however, the performance ratio between HD and TH models, as well as between DD and ET models, is slightly worse, due to the larger sensitivity of the device behavior to the lattice temperature. Conversely, since the coupling among carrier energy-balance and continuity equations is weaker, the overall performance of the TH model, with respect to the DD scheme, improves.
The practicality of the TH model, as well as the completeness of the provided physical picture, is hence demonstrated.

References

[1] S. Szeto and R. Reif, "A unified electrothermal hot-carrier transport model for silicon bipolar transistor simulations," *Solid State Electronics*, vol. 32, pp. 307–315, 1989.

[2] A. Benvenuti, G. Ghione, M. Pinto, W. Coughran, and N. Schryer, "Coupled thermal-fully hydrodynamic simulation of InP-based HBTs," in *Proceedings of the IEDM 92 Conf.*, (San Francisco), pp. 737–740, 1992.

[3] K. Katayama and T. Toyabe, "A new hot carrier simulation method based on full 3D hydrodynamic equations," in *Proceedings of the IEDM 89 Conf.*, (Washington D.C), pp. 135–138, 1989.

[4] A. Pierantoni, P. Ciampolini, A. Gnudi, and G. Baccarani, "Three-dimensional evaluation of substrate current in recessed-oxide MOSFETs," *IEICE Trans. Electron.*, vol. E75-C, no. 2, pp. 181–188, 1992.

[5] P. Conti, N. Hitschfeld, and W. Fichtner, "OMEGA-an octree-based mixed element grid allocator for the simulation of complex 3D device structures," *IEEE Trans. on CAD of ICAS*, vol. CAD-10, pp. 1231–1241, 1991.

[6] A. Pierantoni, P. Ciampolini, and G. Baccarani, "Accurate modeling of electrothermal effects in silicon devices," in *Proceedings of the ESSDERC XXII Conf.*, (Lovanio), pp. 769–772, 1992.

[1] In table 2, abbreviations HCC and HEB indicate hole continuity equations and hole energy balance equations, respectively

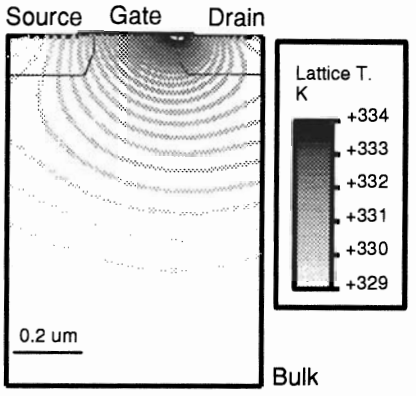

Fig. 1: Lattice temperature in the MOSFET ($V_{GS} = V_{DS} = 2$V).

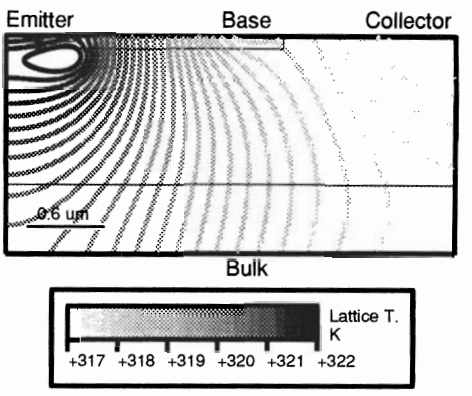

Fig. 2: Lattice temperature in the BJT ($V_C = 3$V, $V_{BE} = 0.95$V).

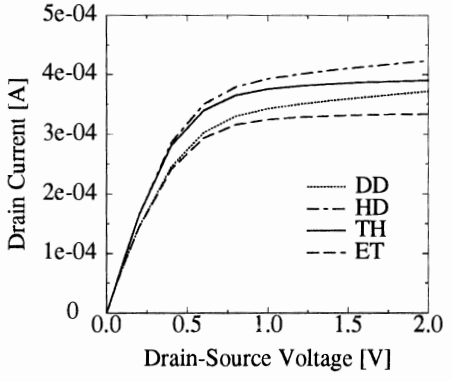

Fig. 3: MOSFET drain current comparison. ($V_{GS} = 2$V).

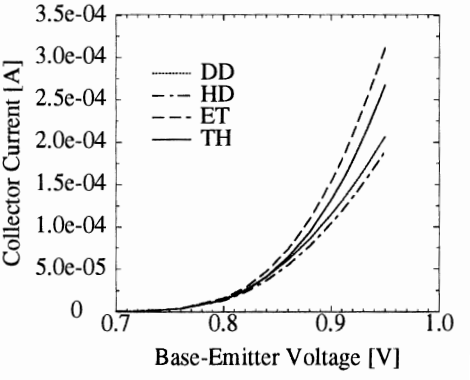

Fig. 4: BJT collector current comparison. ($V_C = 3$V).

Scheme	Block partition	Gummel Iterations	Normalized CPU time
DD	[POI,ECC]	-	1
ET	[POI,ECC] [LEB]	4	1.96
HD	[POI,ECC] [EEB]	18	4.63
TH three-block	[POI,ECC] [EEB] [LEB]	217	32.35
TH two-block	[POI,ECC] [EEB,LEB]	18	5.86

Table 1: MOS transistor

Scheme	Block partition	Gummel Iterations	Normalized CPU time
DD	[POI,ECC,HCC]	-	1
ET	[POI,ECC,HCC] [LEB]	6	2.25
HD	[POI,ECC,HCC] [EEB] [HEB]	17	2.35
TH	[POI,ECC,HCC] [EEB,HEB,LEB]	18	3.98

Table 2: bipolar transistor